Simple-Averaging Gradient Recovery and Error Estimation for the Steklov Eigenvalue Problem

Original Research Article

Abstract

The Steklov eigenvalue problem is an elliptic eigenvalue problem in which the spectral parameter appears in the boundary condition. This paper examines its continuous piecewise linear finite element approximation and a classical equal-weight nodal gradient recovery. The contribution lies in a Steklov-specific analysis connecting recovered-gradient superconvergence, a computable error estimator, and eigenvalue postprocessing, rather than in a new recovery formula. Under specified regularity and local mesh-structure assumptions, the recovered gradient has an error of order $O(h^{1+\alpha_0})$, where $0 < \alpha_0 \leq 1/2$. The eigenvalue error identity yields $\lambda_h - \lambda = \eta_h^2 + O(h^{2+\alpha_0})$ for the recovery-based estimator η_h. For the first isolated simple eigenvalue, asymptotic exactness follows under the additional nondegeneracy condition $\lambda_h - \lambda \geq c_0 h^2$. The postprocessed eigenvalue $\widehat{\lambda}_h = \lambda_h - \eta_h^2$ has an error bound of order $O(h^{2+\alpha_0})$. Numerical experiments on the unit square with uniform and smoothly perturbed triangular meshes, and on an additional rectangular domain with uniform triangular meshes, support the predicted eigenvalue and recovered-gradient convergence trends and demonstrate the estimator's effectivity. The observed postprocessed eigenvalue errors are smaller than the corresponding uncorrected errors in the tested cases, although they are not strictly monotone under mesh refinement.

Keywords: Steklov eigenvalue problem; linear finite elements; equal-weight gradient recovery; superconvergence; a posteriori error estimator; asymptotic exactness; eigenvalue postprocessing.

2020 Mathematics Subject Classification: 35P15; 65N25; 65N30.

1 Introduction

1.1 Research Background and Significance

Eigenvalue problems arise in many applications of partial differential equations. The Steklov eigenvalue problem is distinguished by the appearance of the spectral parameter in the boundary condition. The model problem is

$$\begin{cases} -\Delta u + \kappa^2 u = 0, & x \in \Omega, \\ \dfrac{\partial u}{\partial n} = \lambda u, & x \in \partial\Omega, \end{cases} \tag{1.1}$$

where $\Omega \subset \mathbb{R}^2$ is a bounded polygonal domain, n is the unit outward normal, $\kappa > 0$, and (λ, u) is an eigenpair. The corresponding variational formulation contains a boundary bilinear form, so the approximation of the eigenfunction on $\partial\Omega$ also enters the error analysis.

For continuous piecewise linear finite elements on triangular meshes, u_h is continuous, whereas ∇u_h is piecewise constant and generally discontinuous across element interfaces. The classical equal-weight simple-averaging gradient recovery operator is employed, in which the element gradients in each nodal patch are averaged with identical weights (Hlaváček et al., 1996). The appeal of this recovery is its simplicity: it requires neither local polynomial fitting nor element-area weighting. The focus of the present analysis is on its Steklov-specific superconvergence and on how the recovered gradient can be used for eigenvalue error estimation and postprocessing.

1.2 Related Work

Finite element approximation of symmetric elliptic eigenvalue problems has been extensively studied; Boffi provides a systematic account of spectral approximation and convergence theory (Boffi, 2010). For the Steklov problem, the spectral parameter occurs in the boundary condition, and error analysis must account for both domain approximation and boundary errors. Bi et al. established error estimates for linear triangular finite element approximations, including conforming and nonconforming methods (Bi et al., 2018). These results provide a basis for the finite element analysis in Section 2.

Gradient recovery is a postprocessing technique for improving finite element derivative approximations. The superconvergent patch recovery method of Zienkiewicz and Zhu uses element information around mesh nodes to construct a recovered gradient (Zienkiewicz and Zhu, 1992). Hlaváček, Křížek, and Pištora studied a simple averaging formula for recovering gradients of linear finite elements and established superconvergence properties on suitable triangulations (Hlaváček et al., 1996). Xu and Zhang analyzed recovery-type estimators on mildly structured grids and highlighted the role of local mesh geometry in superconvergence (Xu and Zhang, 2004).

Recovery techniques have also been applied to eigenvalue problems. Mao, Shen, and Zhou studied adaptive algorithms using local-averaging a posteriori estimators (Mao et al., 2006), while Naga, Zhang, and Zhou used polynomial-preserving recovery to improve eigenvalue approximations (Naga et al., 2006). For the scalar Steklov problem, Armentano and Padra analyzed a residual-type a posteriori estimator (Armentano and Padra, 2008), while Xiong et al. developed residual-based a posteriori and superconvergence analysis with postprocessing through an auxiliary source problem (Xiong et al., 2023). Recent work has also investigated residual-type adaptive estimation for a Steklov eigenvalue problem associated with the Lamé operator in elasticity (Li and Zhang, 2024); that vector-valued problem differs from the scalar model considered here. Zhang and Han considered asymptotically exact recovery-based estimators for nonsymmetric elliptic eigenvalue problems (Zhang and Han, 2025).

The present work builds on the classical equal-weight simple-averaging recovery operator rather than introducing a new recovery formula. Its contribution is to develop, for the Steklov eigenvalue problem, a unified analysis that connects recovered-gradient superconvergence with a computable eigenvalue-error estimator, proves asymptotic exactness under a nondegeneracy condition, and derives a recovery-based postprocessed eigenvalue. The analysis explicitly accounts for the boundary spectral term characteristic of the Steklov problem and is carried out under specified regularity and local mesh-structure assumptions. In particular, the recovery formula itself is not claimed to be new, and asymptotic exactness is conditional on an additional eigenvalue-error lower bound.

1.3 Main Contributions

Building on the classical simple-averaging recovery operator, this paper develops a Steklov-specific framework for gradient superconvergence, eigenvalue error estimation, asymptotic exactness, and eigenvalue postprocessing. The main contributions are as follows.

First, under suitable regularity and local mesh-structure assumptions, the recovered gradient is

shown to satisfy the superconvergence estimate

$$\|G_h u_h - \nabla u\|_{0,\Omega} \le C h^{1+\alpha_0}, \qquad 0 < \alpha_0 \le \frac{1}{2}.$$

Second, a computable recovery-based error estimator is defined by

$$\eta_h = \|G_h u_h - \nabla u_h\|_{0,\Omega}.$$

Combining the superconvergence result with the eigenvalue error identity yields

$$\lambda_h - \lambda = \eta_h^2 + O(h^{2+\alpha_0}).$$

Moreover, for the first isolated simple Steklov eigenvalue, under the additional nondegeneracy condition

$$\lambda_h - \lambda \ge c_0 h^2,$$

the estimator is asymptotically exact:

$$\frac{\eta_h^2}{\lambda_h - \lambda} = 1 + O(h^{\alpha_0}).$$

Finally, a postprocessed eigenvalue is defined by

$$\widehat{\lambda}_h = \lambda_h - \eta_h^2,$$

and the following error estimate is established:

$$|\widehat{\lambda}_h - \lambda| \le C h^{2+\alpha_0}.$$

1.4 Organization of the Paper

Section 2 presents the variational formulation, finite element discretization, a priori error estimates, and eigenvalue error identity. Section 3 defines the simple-averaging recovery operator and establishes its superconvergence, estimator exactness, and postprocessed eigenvalue estimate. Section 4 reports numerical experiments on the unit square and an additional rectangular domain, including tests of convergence, estimator performance, and eigenvalue postprocessing on the considered mesh families. Section 5 concludes the paper and discusses possible extensions.

2 Steklov Eigenvalue Problem and Its Finite Element Approximation

Starting from the Steklov problem in Section 1, the weak formulation and linear finite element approximation are introduced, followed by eigenfunction and eigenvalue error estimates needed for the recovery analysis in Section 3.

2.1 Basic Notation

Let $\Omega \subset \mathbb{R}^2$ be a bounded polygonal domain with boundary $\partial\Omega$. For a nonnegative integer m, define

$$H^m(\Omega) = \left\{ v \in L^2(\Omega) \mid D^\alpha v \in L^2(\Omega),\ |\alpha| \le m \right\}.$$

The corresponding norm and seminorm are

$$\|v\|_{m,\Omega} = \left(\sum_{|\alpha| \le m} \|D^\alpha v\|_{0,\Omega}^2 \right)^{1/2}, \qquad |v|_{m,\Omega} = \left(\sum_{|\alpha| = m} \|D^\alpha v\|_{0,\Omega}^2 \right)^{1/2}.$$

For $m = 0$, the notation is

$$(u, v)_\Omega = \int_\Omega uv\, dx, \qquad \|v\|_{0,\Omega} = (v, v)_\Omega^{1/2}.$$

On $\partial\Omega$, let

$$\langle u, v\rangle_{\partial\Omega} = \int_{\partial\Omega} uv\, ds, \qquad \|v\|_{0,\partial\Omega} = \langle v, v\rangle_{\partial\Omega}^{1/2}.$$

For vector fields $\boldsymbol{p}, \boldsymbol{q} \in [L^2(\Omega)]^2$, the L^2 inner product and norm are

$$(\boldsymbol{p}, \boldsymbol{q})_\Omega = \int_\Omega \boldsymbol{p} \cdot \boldsymbol{q}\, dx, \qquad \|\boldsymbol{p}\|_{0,\Omega} = (\boldsymbol{p}, \boldsymbol{p})_\Omega^{1/2}.$$

Set $V = H^1(\Omega)$ and define

$$\begin{aligned} a(u, v) &= \int_\Omega \left(\nabla u \cdot \nabla v + \kappa^2 uv\right)\, dx, \\ b(u, v) &= \int_{\partial\Omega} uv\, ds. \end{aligned} \tag{2.1}$$

Both forms are symmetric. Since $\kappa > 0$,

$$a(v, v) = \|\nabla v\|_{0,\Omega}^2 + \kappa^2 \|v\|_{0,\Omega}^2 \geq \min\{1, \kappa^2\} \|v\|_{1,\Omega}^2,$$

so $a(\cdot, \cdot)$ is coercive and defines the energy norm $\|v\|_a = a(v, v)^{1/2}$. The trace theorem gives

$$\|v\|_{0,\partial\Omega} \leq C\|v\|_{1,\Omega}, \qquad v \in H^1(\Omega),$$

and hence $b(\cdot, \cdot)$ is continuous on $H^1(\Omega)$. Throughout, C denotes a positive constant independent of h, which may vary between occurrences.

2.2 The Steklov Eigenvalue Problem and Its Weak Formulation

For arbitrary $v \in H^1(\Omega)$, multiplying the interior equation in (1.1) by v, integrating over Ω, and applying Green's formula together with $\partial u/\partial n = \lambda u$ gives

$$\int_\Omega \left(\nabla u \cdot \nabla v + \kappa^2 uv\right)\, dx = \lambda \int_{\partial\Omega} uv\, ds.$$

Thus, the weak problem is to find $(\lambda, u) \in \mathbb{R} \times V$, with $u \neq 0$, such that

$$a(u, v) = \lambda b(u, v), \qquad \forall v \in V. \tag{2.2}$$

Since an eigenfunction is determined up to a nonzero multiplicative constant, the boundary normalization is imposed:

$$b(u, u) = \|u\|_{0,\partial\Omega}^2 = 1. \tag{2.3}$$

Taking $v = u$ in (2.2) yields

$$\lambda = a(u, u) = \|\nabla u\|_{0,\Omega}^2 + \kappa^2 \|u\|_{0,\Omega}^2.$$

2.3 Finite Element Discretization

Let $\mathcal{T}_h$ be a shape-regular triangulation of Ω, with

$$h = \max_{K \in \mathcal{T}_h} h_K,$$

where h_K is the diameter of K. Define the continuous piecewise linear finite element space

$$V_h = \left\{v_h \in C(\overline{\Omega}) \mid v_h|_K \in P_1(K),\ \forall K \in \mathcal{T}_h\right\} \subset V, \tag{2.4}$$

where $P_1(K)$ is the space of linear polynomials on K. The discrete eigenvalue problem is to find $(\lambda_h, u_h) \in \mathbb{R} \times V_h$, with $u_h \neq 0$, such that

$$a(u_h, v_h) = \lambda_h b(u_h, v_h), \qquad \forall v_h \in V_h. \tag{2.5}$$

The boundary normalization is imposed:

$$b(u_h, u_h) = \|u_h\|^2_{0,\partial\Omega} = 1. \tag{2.6}$$

Taking $v_h = u_h$ gives

$$\lambda_h = a(u_h, u_h) = \|\nabla u_h\|^2_{0,\Omega} + \kappa^2 \|u_h\|^2_{0,\Omega}.$$

Let $\{z_i\}_{i=1}^N$ and $\{\phi_i\}_{i=1}^N$ be the mesh nodes and their nodal basis functions. Writing

$$u_h = \sum_{i=1}^{N} U_i \phi_i, \qquad \boldsymbol{U} = (U_1, U_2, \ldots, U_N)^T,$$

and testing (2.5) with each ϕ_i yields

$$A\boldsymbol{U} = \lambda_h B\boldsymbol{U}, \tag{2.7}$$

where

$$A_{ij} = a(\phi_j, \phi_i), \qquad B_{ij} = b(\phi_j, \phi_i).$$

2.4 A Priori Error Estimates for the Finite Element Approximation

Let (λ, u) be an isolated simple eigenpair and (λ_h, u_h) its corresponding finite element eigenpair for sufficiently small h. Assume that both eigenfunctions are boundary-normalized, their signs are chosen consistently, $u \in H^2(\Omega)$, and the associated dual problem has H^2 regularity. Let $I_h u \in V_h$ be the nodal interpolant. Standard interpolation and spectral approximation estimates for isolated simple eigenvalues (see, e.g., Boffi, 2010; Bi et al., 2018) give

$$\|u - I_h u\|_{0,\Omega} + h\|u - I_h u\|_{1,\Omega} \leq Ch^2 \|u\|_{2,\Omega}. \tag{2.8}$$

The energy- and L^2-error estimates are

$$\|u - u_h\|_{1,\Omega} \leq Ch\|u\|_{2,\Omega}, \tag{2.9}$$

and, by the duality argument,

$$\|u - u_h\|_{0,\Omega} \leq Ch^2 \|u\|_{2,\Omega}. \tag{2.10}$$

The multiplicative trace inequality states that

$$\|v\|^2_{0,\partial\Omega} \leq C\left(\|v\|_{0,\Omega}\|\nabla v\|_{0,\Omega} + \|v\|^2_{0,\Omega}\right), \qquad v \in H^1(\Omega). \tag{2.11}$$

Setting $e = u - u_h$ and applying (2.9)–(2.10) yields

$$\begin{aligned} \|e\|^2_{0,\partial\Omega} &\leq C\left(\|e\|_{0,\Omega}\|\nabla e\|_{0,\Omega} + \|e\|^2_{0,\Omega}\right) \\ &\leq C(h^3 + h^4)\|u\|^2_{2,\Omega} \leq Ch^3 \|u\|^2_{2,\Omega}. \end{aligned}$$

Consequently,

$$\|u - u_h\|_{0,\partial\Omega} \leq Ch^{3/2} \|u\|_{2,\Omega}. \tag{2.12}$$

2.5 An Eigenvalue Error Identity

The following identity relates the eigenvalue error to the eigenfunction error.

Lemma 2.1. *Let (λ, u) and (λ_h, u_h) be corresponding exact and discrete eigenpairs satisfying $b(u, u) = b(u_h, u_h) = 1$. With $e = u - u_h$, the following identity holds:*

$$\lambda_h - \lambda = a(e, e) - \lambda b(e, e). \tag{2.13}$$

Proof. The eigenvalue equations and normalization give

$$\lambda = a(u,u), \qquad \lambda_h = a(u_h,u_h).$$

Since $u_h = u - e$, symmetry of $a(\cdot,\cdot)$ yields

$$\lambda_h - \lambda = a(e,e) - 2a(u,e).$$

Taking $v = e$ in the continuous eigenvalue equation gives $a(u,e) = \lambda b(u,e)$. Moreover, the normalization conditions imply

$$b(e,e) = b(u-u_h, u-u_h) = 2 - 2b(u,u_h) = 2b(u,e).$$

Hence $2a(u,e) = \lambda b(e,e)$, and substitution proves the identity. □

By the definitions of $a(\cdot,\cdot)$ and $b(\cdot,\cdot)$, (2.13) becomes

$$\lambda_h - \lambda = \|\nabla e\|_{0,\Omega}^2 + \kappa^2\|e\|_{0,\Omega}^2 - \lambda\|e\|_{0,\partial\Omega}^2, \qquad e = u - u_h. \tag{2.14}$$

The estimates above imply

$$\|\nabla e\|_{0,\Omega}^2 = O(h^2), \qquad \|e\|_{0,\Omega}^2 = O(h^4), \qquad \|e\|_{0,\partial\Omega}^2 = O(h^3).$$

Thus, the last two terms in (2.14) are of higher order, and

$$\lambda_h - \lambda = \|\nabla(u-u_h)\|_{0,\Omega}^2 + O(h^3). \tag{2.15}$$

Taking absolute values in (2.14) and using the same estimates gives

$$\begin{aligned} |\lambda_h - \lambda| &\le \|\nabla e\|_{0,\Omega}^2 + \kappa^2\|e\|_{0,\Omega}^2 + |\lambda|\|e\|_{0,\partial\Omega}^2 \\ &\le C(h^2 + h^4 + h^3) \le Ch^2. \end{aligned}$$

Therefore,

$$|\lambda_h - \lambda| \le Ch^2. \tag{2.16}$$

This is an upper bound and does not provide a second-order lower bound. For the first eigenvalue, the conforming min–max principle gives $\lambda_h \ge \lambda$, but does not ensure $\lambda_h - \lambda \ge c_0 h^2$. This nondegeneracy condition, with $c_0 > 0$ independent of h, is therefore imposed as an additional assumption in the asymptotic exactness theorem in Section 3. Together with (2.16), it gives an eigenvalue error of order h^2. Relation (2.15) identifies the squared gradient error as the leading term and motivates the recovery-based estimator studied in Section 3.

3 Simple-Averaging Gradient Recovery and Error Estimation

Building on the finite element approximation theory established in Section 2, this section investigates a simple-averaging gradient recovery method for the Steklov eigenvalue problem and the associated error estimates. An equal-weight gradient recovery operator and its basic properties are introduced first. Superconvergence is then analyzed under specified local mesh structures using an interpolation superapproximation lemma. Finally, a computable recovery-based estimator is constructed and related to the Steklov eigenvalue error identity.

3.1 The Simple-Averaging Gradient Recovery Operator

Let $\mathcal{T}_h$ be a triangulation of Ω, and let V_h be the continuous piecewise linear finite element space defined in Section 2. Since $v_h|_K \in P_1(K)$ for every $v_h \in V_h$, its gradient is constant on each element K, but is generally discontinuous across element interfaces.

For a mesh node z, define its nodal patch and the number of elements in the patch by

$$\omega_z = \{K \in \mathcal{T}_h : \, z \in \overline{K}\}, \qquad N_z = \#\omega_z.$$

The simple-averaging recovered gradient at z is

$$G_h v_h(z) = \frac{1}{N_z} \sum_{K \in \omega_z} \nabla v_h|_K, \qquad v_h \in V_h.$$

Thus, every element in the nodal patch receives the same weight $1/N_z$; no element-area weighting or local polynomial fitting is used. Here, $G_h v_h$ denotes the recovery of the elementwise gradient of v_h.

Let $\{\phi_z\}$ be the nodal basis of V_h. Extending the recovered nodal values by linear interpolation gives

$$G_h v_h(x) = \sum_z G_h v_h(z) \phi_z(x) \in [V_h]^2.$$

Hence, $G_h v_h$ is a continuous piecewise linear vector field obtained by element-gradient evaluation, equal-weight nodal averaging, and nodal interpolation.

3.2 Basic Properties of the Recovery Operator and Mesh Assumptions

The linearity and stability of G_h are recorded before the local mesh conditions used in the superconvergence analysis.

3.2.1 Linearity

By the definition of G_h, for any $v_h, w_h \in V_h$ and $c_1, c_2 \in \mathbb{R}$,

$$G_h(c_1 v_h + c_2 w_h) = c_1 G_h v_h + c_2 G_h w_h.$$

In particular, $G_h(v_h - w_h) = G_h v_h - G_h w_h$.

3.2.2 Stability

Assume that $\mathcal{T}_h$ is shape-regular and quasi-uniform. Then the number of elements in each nodal patch is uniformly bounded. Jensen's inequality gives, for every node z,

$$|G_h v_h(z)|^2 \le \frac{1}{N_z} \sum_{K \in \omega_z} \left| \nabla v_h|_K \right|^2.$$

For an element K, let $\mathcal{N}(K)$ be its three vertices. Local norm equivalence for piecewise linear functions yields

$$\|G_h v_h\|_{0,K}^2 \le C|K| \sum_{z \in \mathcal{N}(K)} |G_h v_h(z)|^2.$$

Summing over $\mathcal{T}_h$, and using the comparability of element areas within each nodal patch and the uniformly bounded overlap of the patches, one obtains

$$\begin{aligned} \|G_h v_h\|_{0,\Omega}^2 &\le C \sum_{K \in \mathcal{T}_h} |K| \sum_{z \in \mathcal{N}(K)} \frac{1}{N_z} \sum_{K' \in \omega_z} \left| \nabla v_h|_{K'} \right|^2 \\ &\le C \sum_{K' \in \mathcal{T}_h} |K'| \left| \nabla v_h|_{K'} \right|^2 = C \|\nabla v_h\|_{0,\Omega}^2. \end{aligned}$$

Consequently,

$$\|G_h v_h\|_{0,\Omega} \le C \|\nabla v_h\|_{0,\Omega}, \qquad v_h \in V_h,$$

where C is independent of h. This stability estimate alone does not imply superconvergence: on a general unstructured mesh, simple averaging need not improve the convergence order. The following local mesh conditions are therefore imposed.

3.2.3 Local Mesh Structure Assumptions

Let $\{\mathcal{T}_h\}$ be a family of shape-regular, quasi-uniform triangulations of the fixed polygonal domain Ω, and set

$$h = \max_{K \in \mathcal{T}_h} h_K.$$

Let $\mathcal{N}_h^\circ$ denote the set of interior nodes. For an interior node z, enumerate the triangles in ω_z counterclockwise as

$$K_i = \triangle(z, x_i, x_{i+1}), \qquad i = 1, \dots, N_z,$$

with cyclic indices. For the adjacent pair K_i, K_{i+1}, write the vertices of their union in boundary order as

$$A_i = x_i, \qquad B_i = x_{i+1}, \qquad C_i = x_{i+2}, \qquad D_i = z.$$

The node z is called regular if, for some fixed $0 < \alpha \leq 1$ and a constant C independent of z and h,

$$|A_i + C_i - B_i - D_i| = |x_i + x_{i+2} - x_{i+1} - z| \leq Ch^{1+\alpha}, \quad i = 1, \dots, N_z. \tag{3.1}$$

Let $\mathcal{Z}_{1,h}$ be the set of regular interior nodes and let

$$\mathcal{Z}_{2,h} = \mathcal{N}_h^\circ \setminus \mathcal{Z}_{1,h}.$$

Define the exceptional region

$$\Omega_{2,h} = \bigcup_{z \in \mathcal{Z}_{2,h}} \bigcup_{K \in \omega_z} \overline{K},$$

and assume

$$|\Omega_{2,h}| \leq Ch^{\sigma_0}, \qquad \sigma_0 > 0. \tag{3.2}$$

Set

$$\alpha_0 = \min\left\{\alpha, \frac{\sigma_0}{2}, \frac{1}{2}\right\}. \tag{3.3}$$

Let $\Omega_{\partial,h}$ be the union of elements containing boundary nodes. Shape regularity and quasi-uniformity on the fixed polygonal domain imply

$$|\Omega_{\partial,h}| \leq Ch. \tag{3.4}$$

Writing $\mathcal{Z}_{\partial,h}$ for the boundary nodes, partition the mesh into

$$\mathcal{T}_{2,h} = \{K \in \mathcal{T}_h : \mathcal{N}(K) \cap (\mathcal{Z}_{2,h} \cup \mathcal{Z}_{\partial,h}) \neq \varnothing\},$$
$$\mathcal{T}_{1,h} = \mathcal{T}_h \setminus \mathcal{T}_{2,h}.$$

Thus,

$$\mathcal{T}_h = \mathcal{T}_{1,h} \cup \mathcal{T}_{2,h}, \qquad \mathcal{T}_{1,h} \cap \mathcal{T}_{2,h} = \varnothing.$$

If

$$\widetilde{\Omega}_{2,h} = \bigcup_{K \in \mathcal{T}_{2,h}} \overline{K} = \Omega_{2,h} \cup \Omega_{\partial,h}, \qquad \widetilde{\sigma}_0 = \min\{\sigma_0, 1\},$$

then (3.2) and (3.4) give

$$|\widetilde{\Omega}_{2,h}| \leq C(h^{\sigma_0} + h) \leq Ch^{\widetilde{\sigma}_0}.$$

Every node of an element in $\mathcal{T}_{1,h}$ is a regular interior node. Hence, for any two adjacent elements in $\mathcal{T}_{1,h}$ sharing an edge, their union satisfies the approximate parallelogram condition (3.1) at either endpoint of the common edge. The resulting partition therefore satisfies the $(\alpha, \widetilde{\sigma}_0)$ mesh condition of Xu and Zhang, with

$$\min\left\{\alpha, \frac{\widetilde{\sigma}_0}{2}, \frac{1}{2}\right\} = \min\left\{\alpha, \frac{\sigma_0}{2}, \frac{1}{2}\right\} = \alpha_0.$$

For a symmetric matrix $H \in \mathbb{R}^{2\times 2}$, define

$$q_{z,H}(x) = \frac{1}{2}(x - z)^T H (x - z),$$

and let $I_K q_{z,H}$ be its local linear Lagrange interpolant on K. The Frobenius norm is defined by

$$\|H\|_F = \left(\sum_{i,j=1}^{2} |H_{ij}|^2 \right)^{1/2}.$$

The following local cancellation property is the key geometric estimate for the recovery analysis.

Lemma 3.1 (Local cancellation estimate under the approximate parallelogram condition)**.** *Let $\mathcal{T}_h$ be shape-regular and quasi-uniform, and let $z \in \mathcal{Z}_{1,h}$ be a regular interior node satisfying* (3.1) *throughout ω_z. For sufficiently small h, the patch ω_z consists of six triangles. Moreover, for every symmetric matrix $H \in \mathbb{R}^{2\times 2}$,*

$$\left| \frac{1}{N_z} \sum_{K \in \omega_z} \nabla I_K q_{z,H} \right| \leq C h^{1+\alpha} \|H\|_F, \tag{3.5}$$

where C is independent of h.

Proof. Write

$$r_i = x_i - z, \qquad e_i = r_i + r_{i+2} - r_{i+1}.$$

By (3.1),

$$|e_i| \leq C h^{1+\alpha}, \qquad i = 1, \dots, N_z, \tag{3.6}$$

and hence $r_{i+2} = r_{i+1} - r_i + e_i$. Shape regularity and quasi-uniformity imply that the number of elements in ω_z is uniformly bounded and

$$c \leq \frac{|r_i|}{h} \leq C, \qquad \det(r_i, r_{i+1}) \geq c h^2.$$

To prove that $N_z = 6$ for sufficiently small h, suppose to the contrary that there exist $h_j \to 0$ and regular interior nodes z_j for which the patch cardinality is a fixed integer $N_* \neq 6$. Such a constant-cardinality subsequence exists because shape regularity gives a uniform upper bound on the number of triangles meeting an interior vertex. The normalized vectors

$$\xi_i^{(j)} = \frac{r_i^{(j)}}{h_j}, \qquad i = 1, \dots, N_*,$$

have a convergent subsequence, and their limits satisfy $\det(\xi_i, \xi_{i+1}) \geq c > 0$. Dividing (3.6) by h_j and taking limits gives

$$\xi_{i+2} = \xi_{i+1} - \xi_i$$

with cyclic indices. Since ξ_1 and ξ_2 are linearly independent, this recurrence has minimal period six. Cyclic closure implies $N_* = 6m$ for some integer $m \geq 1$.

For each j, let $\theta_i^{(j)} \in (0, \pi)$ be the angle at z_j inside the triangle $\triangle(z_j, x_i^{(j)}, x_{i+1}^{(j)})$. Because these nonoverlapping triangles constitute a conforming fan around an interior vertex, their angles cover one full neighborhood of the vertex; in particular,

$$\sum_{i=1}^{N_*} \theta_i^{(j)} = 2\pi.$$

The uniform positive lower determinant bound prevents limiting adjacent vectors from becoming collinear. Thus the limiting oriented angles $\theta_i \in (0, \pi)$ exist and satisfy

$$\sum_{i=1}^{N_*} \theta_i = 2\pi.$$

For $a = \xi_1$ and $b = \xi_2$, one period of the limiting recurrence is

$$a, \quad b, \quad b - a, \quad -a, \quad -b, \quad a - b,$$

followed by a. All successive determinants equal $\det(a,b) > 0$, so every successive counterclockwise angle lies in $(0,\pi)$. The first three such angles carry a to $-a$; their sum is a positive odd multiple of π strictly smaller than 3π, and hence equals π. The last three angles have the same values by simultaneous sign reversal. Therefore every six-vector period has total turning angle 2π.

As $N_* = 6m$, the total limiting angle sum is consequently $2m\pi$. Comparison with the conforming-fan identity above gives $m = 1$ and $N_* = 6$, a contradiction.

The recurrence also gives

$$r_{i+3} = -r_i + e_i + e_{i+1}, \qquad r_{i+4} = -r_{i+1} + e_{i+1} + e_{i+2},$$

and consequently

$$|r_{i+3} + r_i| + |r_{i+4} + r_{i+1}| \le Ch^{1+\alpha}.$$

For $K_i = \triangle(z, x_i, x_{i+1})$, set

$$R_i = \begin{pmatrix} | & | \\ r_i & r_{i+1} \\ | & | \end{pmatrix}, \qquad g_i = \nabla I_{K_i} q_{z,H}.$$

The interpolation conditions yield

$$g_i = \frac{1}{2} R_i^{-T} \begin{pmatrix} r_i^T H r_i \\ r_{i+1}^T H r_{i+1} \end{pmatrix}. \tag{3.7}$$

Define

$$\mathcal{G}_H(r,s) = \frac{1}{2} \begin{pmatrix} r & s \end{pmatrix}^{-T} \begin{pmatrix} r^T H r \\ s^T H s \end{pmatrix}.$$

Then $g_i = \mathcal{G}_H(r_i, r_{i+1})$ and $\mathcal{G}_H(-r,-s) = -\mathcal{G}_H(r,s)$.

By shape regularity and quasi-uniformity, the normalized pairs $(r/h, s/h)$ lie in a uniformly bounded shape-regular set. Since $\mathcal{G}_H(r,s) = h\mathcal{G}_H(r/h, s/h)$, its derivatives with respect to r, s are bounded by $C\|H\|_F$, uniformly in h. Thus $\mathcal{G}_H$ is uniformly Lipschitz with respect to its vertex vectors on the relevant set.

Set

$$\delta_1 = r_{i+3} + r_i, \qquad \delta_2 = r_{i+4} + r_{i+1},$$

so that $|\delta_1| + |\delta_2| \le Ch^{1+\alpha}$. Along the segment

$$p_i(t) = -r_i + t\delta_1, \qquad q_i(t) = -r_{i+1} + t\delta_2, \qquad 0 \le t \le 1,$$

the vector lengths remain of order h, and

$$\det(p_i(t), q_i(t)) = \det(r_i, r_{i+1}) + O(h^{2+\alpha}) \ge \frac{c}{2} h^2$$

for sufficiently small h. The segment therefore remains in a uniformly shape-regular set. The Lipschitz estimate and the oddness of $\mathcal{G}_H$ then imply

$$|g_{i+3} + g_i| = |\mathcal{G}_H(r_{i+3}, r_{i+4}) - \mathcal{G}_H(-r_i, -r_{i+1})| \le Ch^{1+\alpha}\|H\|_F.$$

Pairing g_1 with g_4, g_2 with g_5, and g_3 with g_6, one obtains

$$\left| \sum_{i=1}^{6} g_i \right| \le \sum_{i=1}^{3} |g_{i+3} + g_i| \le Ch^{1+\alpha}\|H\|_F.$$

Since $N_z = 6$, this proves (3.5). □

3.3 Superconvergence of the Recovered Gradient

The following analysis establishes global superconvergence of the recovered gradient under the mesh conditions in Section 3.2. The proof combines an interpolation superapproximation estimate, a supercloseness estimate for the discrete eigenfunction, and a local recovery estimate at regular interior nodes.

Lemma 3.2 (Superapproximation estimate for the finite element interpolation error)**.** *Let $u \in W^{3,\infty}(\Omega)$, and let $\mathcal{T}_h$ satisfy the mesh conditions in Section 3.2. Then, for any $v_h \in V_h$,*

$$|(\nabla(u - I_h u), \nabla v_h)_\Omega| \le Ch^{1+\alpha_0} \|u\|_{W^{3,\infty}(\Omega)} \|v_h\|_{1,\Omega}, \tag{3.8}$$

where α_0 is defined in (3.3)*, and C is independent of h.*

Proof. The mesh partition in Section 3.2 satisfies the $(\alpha, \widetilde{\sigma}_0)$ condition, with $\widetilde{\sigma}_0 = \min\{\sigma_0, 1\}$. Applying Lemma 2.1 of Xu and Zhang (2004) with the piecewise constant matrix $D_K = I$, whose boundedness and adjacent-element variation conditions are immediate, and using $u \in W^{3,\infty}(\Omega) \subset H^3(\Omega) \cap W^{2,\infty}(\Omega)$, gives

$$|(\nabla(u - I_h u), \nabla v_h)_\Omega| \le Ch^{1+\rho} \left(\|u\|_{H^3(\Omega)} + |u|_{W^{2,\infty}(\Omega)} \right) |v_h|_{1,\Omega},$$

where

$$\rho = \min\left\{ \alpha, \frac{\widetilde{\sigma}_0}{2}, \frac{1}{2} \right\} = \alpha_0.$$

Since $|v_h|_{1,\Omega} \le \|v_h\|_{1,\Omega}$ and $\|u\|_{H^3(\Omega)} + |u|_{W^{2,\infty}(\Omega)} \le C\|u\|_{W^{3,\infty}(\Omega)}$, estimate (3.8) follows. □

Lemma 3.3 (Supercloseness estimate for the Steklov finite element eigenfunction)**.** *Let (λ, u) be an isolated simple Steklov eigenpair and (λ_h, u_h) the corresponding discrete eigenpair, with $\kappa > 0$ and $u \in W^{3,\infty}(\Omega)$. Assume*

$$b(u, u) = b(u_h, u_h) = 1,$$

and that the signs of u and u_h are chosen consistently. If the a priori estimates in (2.16) *and* (2.12) *hold, namely,*

$$|\lambda_h - \lambda| \le Ch^2, \qquad \|u - u_h\|_{0,\partial\Omega} \le Ch^{3/2},$$

then

$$\|u_h - I_h u\|_{1,\Omega} \le Ch^{1+\alpha_0}. \tag{3.9}$$

The constant is independent of h and may depend on u and its regularity norm.

Proof. Set $e_h = u_h - I_h u$. Subtracting the continuous and discrete variational equations gives, for any $v_h \in V_h$,

$$\begin{aligned} a(e_h, v_h) = a(u - I_h u, v_h) + (\lambda_h - \lambda) b(u_h, v_h) \\ + \lambda b(u_h - u, v_h). \end{aligned} \tag{3.10}$$

Taking $v_h = e_h$, Lemma 3.2 and the standard interpolation estimate yield

$$|a(u - I_h u, e_h)| \le Ch^{1+\alpha_0} \|e_h\|_{1,\Omega}. \tag{3.11}$$

This uses $h^2 \le h^{1+\alpha_0}$ for $0 < \alpha_0 \le 1/2$ and $0 < h \le 1$.

For the remaining terms, the boundary normalization, the trace inequality, and the two assumed a priori estimates give

$$|(\lambda_h - \lambda) b(u_h, e_h)| \le Ch^2 \|e_h\|_{1,\Omega}, \tag{3.12}$$

and

$$|\lambda b(u_h - u, e_h)| \le Ch^{3/2} \|e_h\|_{1,\Omega}. \tag{3.13}$$

Combining (3.10)–(3.13) and using the coercivity of $a(\cdot,\cdot)$, one obtains

$$c\|e_h\|_{1,\Omega}^2 \le Ch^{1+\alpha_0} \|e_h\|_{1,\Omega},$$

because $\alpha_0 = \min\{\alpha, \sigma_0/2, 1/2\} \le 1/2$ and, for $0 < h \le 1$,

$$h^2 + h^{3/2} \le 2h^{1+\alpha_0}.$$

Dividing by $\|e_h\|_{1,\Omega}$ when $e_h \neq 0$ proves (3.9); the result is immediate if $e_h = 0$. □

Lemma 3.4 (Local recovery error estimate at regular interior nodes)**.** *Let $u \in W^{3,\infty}(\Omega)$, and let $\mathcal{T}_h$ satisfy the shape-regularity, quasi-uniformity, and local mesh conditions in Section 3.2. For the nodal interpolant $I_h u$ and the simple equal-weight averaging recovery operator G_h, there is a constant C independent of h such that, for every regular interior node $z \in \mathcal{Z}_{1,h}$ and sufficiently small h,*

$$|G_h I_h u(z) - \nabla u(z)| \le C h^{1+\alpha} \|u\|_{W^{3,\infty}(\Omega)}. \tag{3.14}$$

Proof. For a regular interior node z, let $H_z = D^2 u(z)$ and $q_{z,H_z}(x) = \frac{1}{2}(x-z)^T H_z (x-z)$. Taylor's formula gives, on the patch ω_z,

$$u(x) = u(z) + \nabla u(z)\cdot(x-z) + q_{z,H_z}(x) + R_z(x), \qquad |R_z(x)| \le C h^3 \|u\|_{W^{3,\infty}(\Omega)}.$$

Since linear interpolation reproduces affine functions,

$$\nabla I_K u = \nabla u(z) + \nabla I_K q_{z,H_z} + \nabla I_K R_z, \qquad K \in \omega_z.$$

The local cancellation estimate in Lemma 3.1 and the bound $\|H_z\|_F \le C\|u\|_{W^{2,\infty}(\Omega)}$ imply

$$\left| \frac{1}{N_z} \sum_{K \in \omega_z} \nabla I_K q_{z,H_z} \right| \le C h^{1+\alpha} \|u\|_{W^{3,\infty}(\Omega)}.$$

Moreover, the local interpolation gradient estimate gives

$$|\nabla I_K R_z| \le C h^{-1} \max_{a \in \mathcal{N}(K)} |R_z(a)| \le C h^2 \|u\|_{W^{3,\infty}(\Omega)}.$$

Averaging these estimates over ω_z and using $h^2 \le h^{1+\alpha}$ for $0 < \alpha \le 1$ proves (3.14). □

For the vector field ∇u, let $I_h(\nabla u)$ denote the vector-valued function obtained by applying nodal linear interpolation to each component.

Theorem 3.1 (Superconvergence of the simple equal-weight averaging recovered gradient)**.** *Let (λ, u) be an isolated simple Steklov eigenpair and (λ_h, u_h) the corresponding discrete eigenpair, with $\kappa > 0$ and $u \in W^{3,\infty}(\Omega)$. Assume that the mesh satisfies the conditions in Section 3.2, that both eigenfunctions are normalized in the boundary L^2 norm, and that their signs are chosen consistently. If the a priori estimates in* (2.16) *and* (2.12) *hold, then*

$$\|G_h u_h - \nabla u\|_{0,\Omega} \le C h^{1+\alpha_0}. \tag{3.15}$$

The constant is independent of h and may depend on u and its regularity norm.

Proof. By linearity of G_h, insert $G_h I_h u$ and $I_h(\nabla u)$ and apply the triangle inequality:

$$\begin{aligned} \|G_h u_h - \nabla u\|_{0,\Omega} \le{}& \|G_h(u_h - I_h u)\|_{0,\Omega} \\ &+ \|G_h I_h u - I_h(\nabla u)\|_{0,\Omega} \\ &+ \|I_h(\nabla u) - \nabla u\|_{0,\Omega}. \end{aligned} \tag{3.16}$$

The stability of G_h and Lemma 3.3 give

$$\|G_h(u_h - I_h u)\|_{0,\Omega} \le C\|u_h - I_h u\|_{1,\Omega} \le C h^{1+\alpha_0}.$$

For the second term, set $w_h = G_h I_h u - I_h(\nabla u)$ and use the partition $\Omega = \Omega_{1,h} \cup \widetilde{\Omega}_{2,h}$ from Section 3.2, up to element boundaries, where

$$\Omega_{1,h} = \bigcup_{K \in \mathcal{T}_{1,h}} \overline{K}.$$

If $K \in \mathcal{T}_{1,h}$, all its vertices z_i are regular interior nodes. Since the nodal basis functions are nonnegative and sum to one, Lemma 3.4 yields

$$|w_h(x)| = \left| \sum_{i=1}^{3} \big(G_h I_h u(z_i) - \nabla u(z_i)\big)\phi_i(x) \right| \le C h^{1+\alpha_0} \|u\|_{W^{3,\infty}(\Omega)}, \quad x \in K.$$

Consequently,

$$\|w_h\|_{0,\Omega_{1,h}} \le Ch^{1+\alpha_0}\|u\|_{W^{3,\infty}(\Omega)}.$$

Now let $K \in \mathcal{T}_{2,h}$. At each vertex z_i of K, if z_i is regular, Lemma 3.4 gives

$$|G_h I_h u(z_i) - \nabla u(z_i)| \le Ch^{1+\alpha}\|u\|_{W^{3,\infty}(\Omega)} \le Ch\|u\|_{W^{3,\infty}(\Omega)}.$$

If z_i is exceptional or lies on the boundary, the standard linear interpolation gradient estimate on each $K' \in \omega_{z_i}$ gives

$$|\nabla I_{K'} u - \nabla u(z_i)| \le Ch\|u\|_{W^{2,\infty}(\Omega)}.$$

Taking the equal-weight average over $K' \in \omega_{z_i}$ gives the same $O(h)$ bound for $|G_h I_h u(z_i) - \nabla u(z_i)|$. Thus, by the partition-of-unity property,

$$|w_h(x)| \le Ch\|u\|_{W^{3,\infty}(\Omega)}, \qquad x \in K,$$

and hence

$$\|w_h\|_{0,\widetilde{\Omega}_{2,h}} \le Ch|\widetilde{\Omega}_{2,h}|^{1/2}\|u\|_{W^{3,\infty}(\Omega)}.$$

The area estimate in Section 3.2 gives $|\widetilde{\Omega}_{2,h}| \le Ch^{\widetilde{\sigma}_0}$, where $\widetilde{\sigma}_0 = \min\{\sigma_0, 1\}$. Since $\alpha_0 \le \widetilde{\sigma}_0/2$, it follows that

$$\|w_h\|_{0,\widetilde{\Omega}_{2,h}} \le Ch^{1+\widetilde{\sigma}_0/2}\|u\|_{W^{3,\infty}(\Omega)} \le Ch^{1+\alpha_0}\|u\|_{W^{3,\infty}(\Omega)}.$$

Combining the two regions, one obtains

$$\|G_h I_h u - I_h(\nabla u)\|_{0,\Omega} \le Ch^{1+\alpha_0}\|u\|_{W^{3,\infty}(\Omega)}. \tag{3.17}$$

Finally, componentwise interpolation of ∇u gives

$$\|I_h(\nabla u) - \nabla u\|_{0,\Omega} \le Ch^2\|u\|_{H^3(\Omega)} \le Ch^{1+\alpha_0}\|u\|_{W^{3,\infty}(\Omega)},$$

because $\alpha_0 \le 1/2$. Substitution of the three bounds into (3.16) proves (3.15). □

3.4 Recovery-Based Error Estimator

Based on the superconvergence result in Theorem 3.1, let

$$e = u - u_h, \qquad \delta_h = G_h u_h - \nabla u_h, \qquad \rho_h = G_h u_h - \nabla u.$$

Then

$$\nabla e = \delta_h - \rho_h.$$

By Theorem 3.1, the following bounds hold:

$$\|\rho_h\|_{0,\Omega} = \|G_h u_h - \nabla u\|_{0,\Omega} \le Ch^{1+\alpha_0}.$$

The recovery-based error estimator is defined by

$$\eta_h = \|G_h u_h - \nabla u_h\|_{0,\Omega} = \|\delta_h\|_{0,\Omega}.$$

Since it depends only on the finite element solution and its recovered gradient, η_h is computable without knowing the exact eigenfunction.

Furthermore, using $\nabla e = \delta_h - \rho_h$ and the reverse triangle inequality, one obtains

$$\begin{aligned} |\eta_h - \|\nabla e\|_{0,\Omega}| &= |\|\delta_h\|_{0,\Omega} - \|\delta_h - \rho_h\|_{0,\Omega}| \\ &\le \|\rho_h\|_{0,\Omega} \\ &\le Ch^{1+\alpha_0}. \end{aligned}$$

Thus, the recovery-based estimator approximates the true finite element gradient error with a higher-order accuracy.

3.5 Recovery Estimate for the Eigenvalue Error

Under the boundary normalization $b(u,u) = b(u_h,u_h) = 1$, the eigenvalue error identity established in Section 2, together with $\nabla e = \delta_h - \rho_h$ and $\eta_h = \|\delta_h\|_{0,\Omega}$, gives

$$\begin{aligned}\lambda_h - \lambda &= \|\delta_h - \rho_h\|_{0,\Omega}^2 + \kappa^2\|e\|_{0,\Omega}^2 - \lambda\|e\|_{0,\partial\Omega}^2 \\ &= \eta_h^2 - 2(\delta_h,\rho_h) + \|\rho_h\|_{0,\Omega}^2 \\ &\quad + \kappa^2\|e\|_{0,\Omega}^2 - \lambda\|e\|_{0,\partial\Omega}^2.\end{aligned}$$

Consequently,

$$\begin{aligned}&|(\lambda_h - \lambda) - \eta_h^2| \\ &\le 2|(\delta_h,\rho_h)| + \|\rho_h\|_{0,\Omega}^2 + \kappa^2\|e\|_{0,\Omega}^2 + |\lambda|\|e\|_{0,\partial\Omega}^2.\end{aligned}$$

By the a priori estimates in Section 2, (2.9), (2.10), and (2.12), together with Theorem 3.1, the following bounds hold:

$$\begin{aligned}\|\nabla e\|_{0,\Omega} &\le Ch, \\ \|e\|_{0,\Omega} &\le Ch^2, \\ \|e\|_{0,\partial\Omega} &\le Ch^{3/2}, \\ \|\rho_h\|_{0,\Omega} &\le Ch^{1+\alpha_0}.\end{aligned}$$

Moreover, since $\delta_h = \nabla e + \rho_h$,

$$\|\delta_h\|_{0,\Omega} \le \|\nabla e\|_{0,\Omega} + \|\rho_h\|_{0,\Omega} \le Ch.$$

Therefore, by the Cauchy–Schwarz inequality,

$$\begin{aligned}&|(\lambda_h - \lambda) - \eta_h^2| \\ &\le C\left(h^{2+\alpha_0} + h^{2+2\alpha_0} + h^4 + h^3\right) \\ &\le Ch^{2+\alpha_0},\end{aligned}$$

where $0 < \alpha_0 \le 1/2$ and $h \le 1$.

Thus, one obtains

$$\lambda_h - \lambda = \eta_h^2 + O(h^{2+\alpha_0}). \tag{3.18}$$

This establishes that the recovery-based estimator approximates the eigenvalue error up to a higher-order term, providing the basis for the asymptotic exactness result in the next section.

3.6 Asymptotic Exactness of the Error Estimator

Theorem 3.2 (Asymptotic exactness of the recovery-based error estimator)**.** *Let (λ,u) be the first isolated simple Steklov eigenpair, and let (λ_h,u_h) be the corresponding first finite element eigenpair. Assume that the hypotheses leading to* (3.18) *hold and that the eigenvalue error satisfies*

$$\lambda_h - \lambda \ge c_0 h^2,$$

where $c_0 > 0$ is independent of h. Then

$$\frac{\eta_h^2}{\lambda_h - \lambda} = 1 + O(h^{\alpha_0}). \tag{3.19}$$

In particular,

$$\lim_{h\to 0}\frac{\eta_h^2}{\lambda_h - \lambda} = 1. \tag{3.20}$$

Proof. By (3.18),

$$\left|(\lambda_h - \lambda) - \eta_h^2\right| \le Ch^{2+\alpha_0}.$$

Together with $\lambda_h - \lambda \ge c_0 h^2$, this gives

$$\begin{aligned}\left|\frac{\eta_h^2}{\lambda_h - \lambda} - 1\right| &= \frac{|\eta_h^2 - (\lambda_h - \lambda)|}{\lambda_h - \lambda} \\ &\le \frac{Ch^{2+\alpha_0}}{c_0 h^2} = Ch^{\alpha_0}.\end{aligned}$$

Since $\alpha_0 > 0$, letting $h \to 0$ proves the result. □

The lower bound in Theorem 3.2 is an additional nondegeneracy hypothesis; it is not a consequence of the conforming min–max inequality $\lambda_h \ge \lambda$ or of the second-order upper bound alone. Without this hypothesis, the absolute estimator expansion (3.18) remains valid, but the stated relative effectivity estimate does not follow from that expansion.

For the first Steklov eigenvalue, the conforming finite element approximation satisfies $\lambda_h \ge \lambda$ by the min–max principle. Define the effectivity index by

$$R_h = \frac{\eta_h^2}{|\lambda_h - \lambda|}. \tag{3.21}$$

Theorem 3.2 therefore implies

$$R_h \longrightarrow 1, \qquad h \to 0.$$

When the exact eigenvalue is unavailable, a sufficiently accurate fine-mesh approximation λ_{ref} can be used to define the numerical effectivity index

$$R_h^{\mathrm{ref}} = \frac{\eta_h^2}{|\lambda_h - \lambda_{\mathrm{ref}}|}. \tag{3.22}$$

This quantity approximates the exact effectivity index only when the reference eigenvalue error is negligible relative to $|\lambda_h - \lambda|$.

To improve eigenvalue accuracy, the postprocessed eigenvalue is defined by

$$\widehat{\lambda}_h = \lambda_h - \eta_h^2. \tag{3.23}$$

Theorem 3.3 (Error estimate for the postprocessed eigenvalue)**.** *Assume that the preceding superconvergence conditions and the eigenvalue error estimate* (3.18) *hold. Then*

$$|\widehat{\lambda}_h - \lambda| \le Ch^{2+\alpha_0}, \tag{3.24}$$

where C is independent of h.

Proof. By (3.23),

$$\widehat{\lambda}_h - \lambda = (\lambda_h - \lambda) - \eta_h^2.$$

The estimate follows directly from (3.18). □

Thus, subtracting the recovery-based estimator cancels the leading term in the original eigenvalue error and improves the convergence order. In particular, when $\alpha_0 = 1/2$, the postprocessed eigenvalue error is $O(h^{5/2})$. Its numerical performance is examined in Section 4.

3.7 Section Summary

This section developed a simple equal-weight averaging gradient recovery operator and established its linearity, stability, and superconvergence properties. Under the prescribed mesh conditions, a local cancellation estimate was combined with the interpolation superapproximation and eigenfunction supercloseness estimates to obtain

$$\|G_h u_h - \nabla u\|_{0,\Omega} \le Ch^{1+\alpha_0}.$$

Based on this result, a recovery-based error estimator was constructed. Combining the superconvergence estimate with the eigenvalue error identity gives

$$\lambda_h - \lambda = \eta_h^2 + O(h^{2+\alpha_0}),$$

which further yields its asymptotic exactness under the nondegeneracy condition. Finally, the postprocessed eigenvalue was shown to satisfy

$$|\widehat{\lambda}_h - \lambda| \le Ch^{2+\alpha_0}.$$

These results provide the theoretical foundation for the numerical experiments in Section 4.

4 Numerical Experiments

4.1 Numerical Model and Experimental Setup

The numerical performance of the simple-averaging gradient recovery method is investigated on the unit square $\Omega = (0,1)^2$, with $\kappa = 1$ in the Steklov problem (1.1).

For this problem, the first eigenvalue and its corresponding eigenfunction are available analytically. Let $\mu = 1/\sqrt{2}$. Then

$$\lambda = \mu \tanh\left(\frac{\mu}{2}\right) \approx 0.240079085427227,$$

and the corresponding eigenfunction is

$$u(x,y) = C\cosh\left(\mu\left(x - \frac{1}{2}\right)\right)\cosh\left(\mu\left(y - \frac{1}{2}\right)\right),$$

where the boundary normalization $\|u\|_{L^2(\partial\Omega)} = 1$ gives

$$C = \left[4\cosh^2\left(\frac{\mu}{2}\right)\left(\frac{1}{2} + \frac{\sinh\mu}{2\mu}\right)\right]^{-1/2}.$$

The problem is discretized using the continuous piecewise linear finite element method described in Section 2. The interior degrees of freedom are eliminated when solving the generalized eigenvalue problem. The discrete eigenfunction is normalized in the boundary L^2 norm, with its sign chosen so that the sum of its boundary nodal values is positive.

The computational mesh is constructed by dividing the unit square into $n \times n$ congruent squares and splitting each square along its lower-left to upper-right diagonal. With $\ell = 1/n$, the maximum element diameter is

$$h = \sqrt{2}\ell = \frac{\sqrt{2}}{n}.$$

Every interior node has six neighboring vertices, and their position vectors satisfy the exact relation

$$r_i + r_{i+2} - r_{i+1} = 0, \qquad i = 1, \ldots, 6,$$

with cyclic indices. Thus, all interior nodes are regular, and

$$\mathcal{Z}_{2,h} = \varnothing, \qquad \Omega_{2,h} = \varnothing.$$

Consequently, the choices $\alpha = 1$ and $\sigma_0 = 1$ are admissible. Together with the boundary-layer estimate $|\Omega_{\partial,h}| \le Ch$, this gives

$$\widetilde{\sigma}_0 = 1, \qquad \alpha_0 = \min\left\{1, \frac{1}{2}, \frac{1}{2}\right\} = \frac{1}{2}.$$

Therefore, Theorem 3.1 yields

$$\|G_h u_h - \nabla u\|_{0,\Omega} \le Ch^{3/2}.$$

The numerical experiments are performed on six successively refined meshes:

$$n = 4,\ 8,\ 16,\ 32,\ 64,\ 128, \qquad h = \frac{\sqrt{2}}{n}.$$

For each mesh, the first discrete eigenvalue λ_h is computed, and the eigenvalue error and recovery-based estimator are defined by

$$E_h = |\lambda_h - \lambda|, \qquad \eta_h^2 = \|G_h u_h - \nabla u_h\|_{0,\Omega}^2.$$

The numerical results are used to examine eigenvalue convergence, gradient superconvergence, estimator exactness, and the accuracy of the postprocessed eigenvalue.

4.2 Convergence of the Steklov Eigenvalues

Table 4.1 reports the absolute errors of the first finite element eigenvalues and the corresponding convergence orders for different mesh sizes.

Table 4.1: Steklov eigenvalue errors and convergence orders

n	Number of nodes	h	$\lvert\lambda_h - \lambda\rvert$	Convergence order
4	25	0.353553	5.6155×10^{-4}	–
8	81	0.176777	1.4720×10^{-4}	1.9317
16	289	0.088388	3.7393×10^{-5}	1.9769
32	1089	0.044194	9.3955×10^{-6}	1.9927
64	4225	0.022097	2.3525×10^{-6}	1.9978
128	16641	0.011049	5.8839×10^{-7}	1.9994

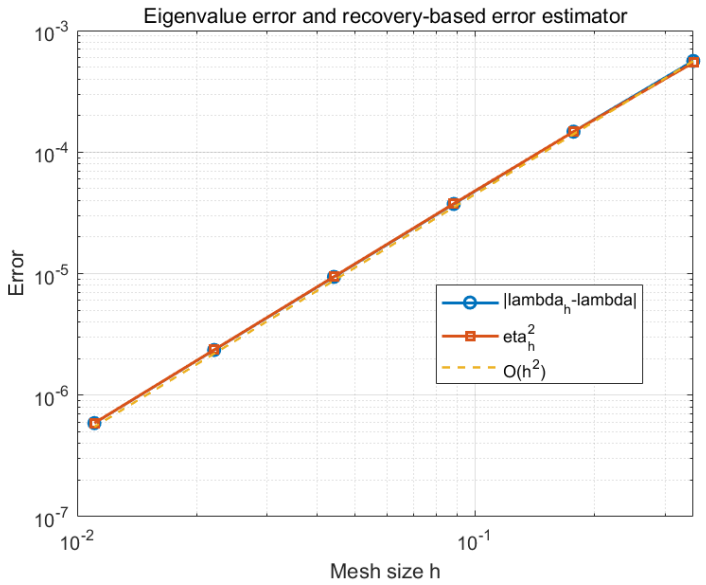


Figure 4.1: Convergence curves of the Steklov eigenvalue error and the recovery-based error estimator

As shown in Table 4.1 and Figure 4.1, the eigenvalue error decreases from 5.6155×10^{-4} to 5.8839×10^{-7} as the mesh is refined, with its convergence order approaching 2. The recovery-based estimator η_h^2 exhibits a similar $O(h^2)$ convergence trend. These results are consistent with the theoretical eigenvalue error estimate in Section 2 and provide a numerical basis for examining the asymptotic exactness of the estimator.

4.3 Convergence of the Recovered Gradient and the Error Estimator

The convergence behavior of the recovery-based error estimator is examined first. Table 4.2 reports the values of η_h^2 and the corresponding convergence orders for different mesh sizes.

Table 4.2: Convergence of the recovery-based error estimator

n	Number of nodes	h	η_h^2	Convergence order
4	25	0.353553	5.4414×10^{-4}	–
8	81	0.176777	1.4713×10^{-4}	1.8869
16	289	0.088388	3.7604×10^{-5}	1.9681
32	1089	0.044194	9.4405×10^{-6}	1.9940
64	4225	0.022097	2.3595×10^{-6}	2.0004
128	16641	0.011049	5.8937×10^{-7}	2.0013

Together with the second-order eigenvalue error estimate in Section 2, the expansion (3.18) is consistent with the approximately second-order behavior of η_h^2 observed in Table 4.2.

To compare the approximation accuracy of the original finite element gradient and the recovered gradient, define

$$E_{\mathrm{FEM},h} = \|\nabla u_h - \nabla u\|_{0,\Omega}, \qquad E_{\mathrm{rec},h} = \|G_h u_h - \nabla u\|_{0,\Omega}.$$

Here, u is the analytical eigenfunction given in Section 4.1, and u_h is the corresponding finite element eigenfunction.

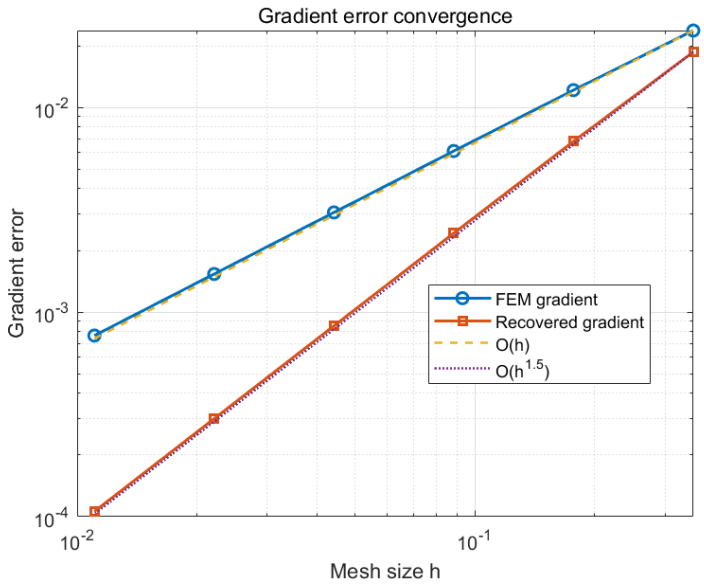


Figure 4.2: Convergence curves of the finite element gradient error and the simple-averaging recovered gradient error

Table 4.3: Errors and convergence orders of the finite element gradient and the simple-averaging recovered gradient

n	Finite element gradient error	Convergence order	Recovered gradient error	Convergence order
4	0.02372875	–	0.01863997	–
8	0.01213839	0.9671	0.006820877	1.4504
16	0.006115842	0.9890	0.002427173	1.4907
32	0.003065338	0.9965	0.0008558509	1.5038
64	0.001533798	0.9989	0.0003011983	1.5066
128	0.0007670653	0.9997	0.0001060611	1.5058

As shown in Table 4.3 and Figure 4.2, the convergence order of the original finite element gradient approaches 1, whereas that of the simple-averaging recovered gradient approaches 1.5. In particular, for $n = 128$, the corresponding errors are 0.0007670653 and 0.0001060611, respectively. The recovered gradient therefore provides a more accurate approximation to the exact gradient. Moreover, its observed convergence rate is consistent with the theoretical estimate in Theorem 3.1, which gives $O(h^{1+\alpha_0})$. Since $\alpha_0 = 1/2$ in the present example, the predicted order is 1.5. These numerical results demonstrate the improved gradient approximation achieved by the simple-averaging recovery method on the uniform triangular meshes considered here.

4.4 Asymptotic Exactness of the Recovery-Based Error Estimator

The effectivity index for evaluating the recovery-based error estimator is defined by

$$R_h = \frac{\eta_h^2}{|\lambda_h - \lambda|}.$$

Since the exact eigenvalue is available for the present model, the denominator can be evaluated directly. The estimator is asymptotically exact if R_h approaches 1 as $h \to 0$.

Table 4.4 reports the effectivity indices on the six successively refined meshes.

Table 4.4: Asymptotic exactness of the recovery-based error estimator

n	Number of nodes	h	η_h^2	R_h
4	25	0.353553	5.4414×10^{-4}	0.96901
8	81	0.176777	1.4713×10^{-4}	0.99954
16	289	0.088388	3.7604×10^{-5}	1.0057
32	1089	0.044194	9.4405×10^{-6}	1.0048
64	4225	0.022097	2.3595×10^{-6}	1.0030
128	16641	0.011049	5.8937×10^{-7}	1.0017

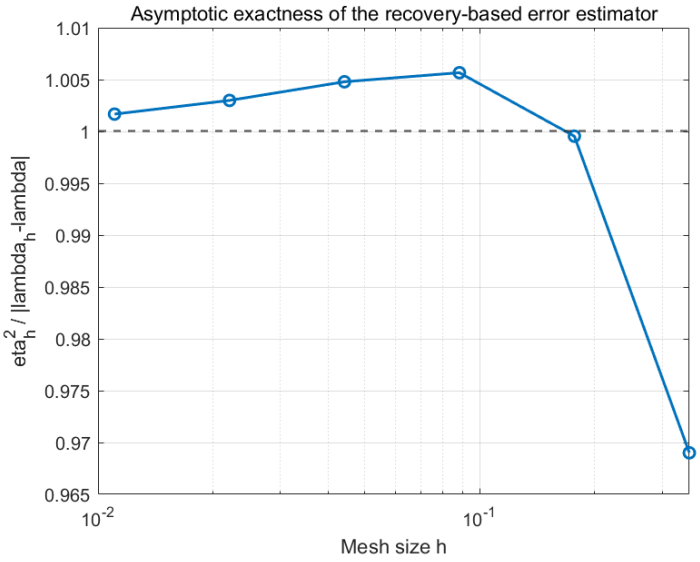


Figure 4.3: Effectivity curve of the recovery-based error estimator

As shown in Table 4.4 and Figure 4.3, the effectivity index remains close to 1 on the refined meshes. Although it is not monotone over all mesh levels, its deviation from 1 decreases steadily from $n = 16$ to $n = 128$. In particular, on the finest mesh, $R_h = 1.0017$, corresponding to a relative deviation of approximately 0.17%. These results provide numerical evidence that the proposed simple-averaging recovery-based error estimator is asymptotically exact for the uniform triangular mesh family considered here, in agreement with the theoretical result in Section 3.

4.5 Postprocessed Eigenvalue Accuracy

To evaluate the eigenvalue-accuracy improvement from gradient recovery, consider the postprocessed eigenvalue defined by

$$\widehat{\lambda}_h = \lambda_h - \eta_h^2. \tag{4.1}$$

Here, η_h^2 is the recovery-based error estimator constructed in Section 3.

Table 4.5 compares the errors and convergence orders of the original and postprocessed eigenvalues on different meshes.

Table 4.5: Errors and convergence orders of the original and postprocessed eigenvalues

h	$\lvert\lambda_h - \lambda\rvert$	Convergence order	$\lvert\widehat{\lambda}_h - \lambda\rvert$	Convergence order
0.353553	5.6155×10^{-4}	–	1.7404×10^{-5}	–
0.176777	1.4720×10^{-4}	1.9317	6.7189×10^{-8}	8.0169
0.088388	3.7393×10^{-5}	1.9769	2.1179×10^{-7}	-1.6563
0.044194	9.3955×10^{-6}	1.9927	4.4995×10^{-8}	2.2348
0.022097	2.3525×10^{-6}	1.9978	7.0415×10^{-9}	2.6758
0.011049	5.8839×10^{-7}	1.9994	9.8348×10^{-10}	2.8399

Note. A negative observed rate indicates an error increase between two successive meshes, not negative asymptotic convergence.

The postprocessed eigenvalue error satisfies

$$|\widehat{\lambda}_h - \lambda| = |(\lambda_h - \lambda) - \eta_h^2|.$$

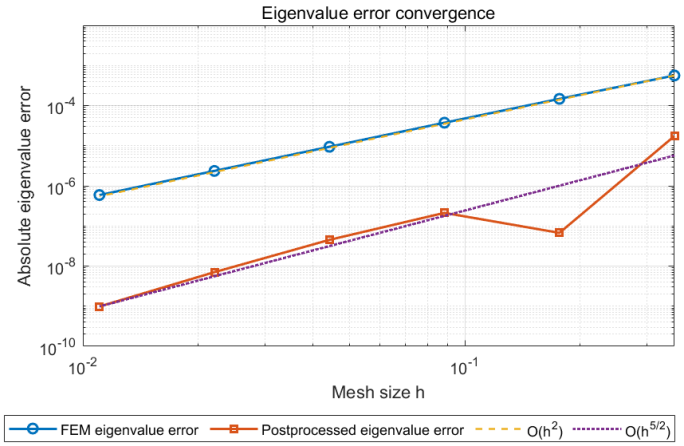


Figure 4.4: Error convergence curves of the original finite element and postprocessed eigenvalues

Table 4.5 and Figure 4.4 show approximately second-order convergence of the original finite element eigenvalue error. The postprocessed error is smaller at each of the six tested mesh levels but is not monotone. In particular, it increases from 6.7189×10^{-8} at $n = 8$ to 2.1179×10^{-7} at $n = 16$. Consequently, the observed rate $\log_2(E_8^{\mathrm{post}}/E_{16}^{\mathrm{post}}) \approx -1.6563$ is negative. This value has been retained in Table 4.5 because it correctly represents the increase in the measured error; it is not an assertion of a negative asymptotic convergence order.

The identity

$$\widehat{\lambda}_h - \lambda = (\lambda_h - \lambda) - \eta_h^2$$

shows that the postprocessed error is the difference of two quantities of order h^2. Near cancellation can make the residual exceptionally small at an individual mesh level, so a subsequent refinement need not yield a smaller absolute residual. The available experiments do not establish whether mesh alignment contributes to this nonmonotonicity; no specific mesh-alignment explanation is claimed.

For subsequent refinements from $n = 16$ to 32, from $n = 32$ to 64, and from $n = 64$ to 128, the observed convergence orders are 2.2348, 2.6758, and 2.8399, respectively. Nevertheless, these values do not yet establish a stable asymptotic convergence rate. According to Theorem 3.3, when $\alpha_0 = 1/2$, the theoretical error bound is $O(h^{5/2})$. The numerical results demonstrate the improvement achieved by the postprocessing procedure, although further mesh refinement and numerical investigation are needed to assess its asymptotic convergence behavior.

4.6 Additional Validation on Smoothly Perturbed Nonuniform Triangular Meshes

To assess whether the observations depend on equal-sized triangles, a second family of triangulations of the same unit square is considered. Each vertex (s, t) of the regular reference grid is mapped to

$$F(s,t) = \big(s + 0.075\sin(\pi s)\sin(\pi t),\ t - 0.060\sin(\pi s)\sin(\pi t)\big).$$

The mapping fixes the boundary of the unit square and produces triangles with unequal sizes and shapes. Since the perturbation is smooth and small, these triangulations remain shape regular and quasi-uniform; the approximate parallelogram residual at regular interior nodes is $O(h^2)$. The same equal-weight recovery operator is used, without retuning its weights. Here h is the largest actual triangle diameter on the perturbed mesh, not the reference-grid value $\sqrt{2}/n$.

Table 4.6: Independent numerical results on smoothly perturbed nonuniform triangular meshes

n	h	$\lvert\lambda_h - \lambda\rvert$	$\lVert G_h u_h - \nabla u\rVert_{0,\Omega}$	$\eta_h^2/\lvert\lambda_h - \lambda\rvert$	$\lvert\widehat{\lambda}_h - \lambda\rvert$
4	0.36731	6.0213×10^{-4}	1.9093×10^{-2}	0.9541	2.7654×10^{-5}
8	0.18449	1.5781×10^{-4}	7.0190×10^{-3}	0.9961	6.1452×10^{-7}
16	0.09235	4.0079×10^{-5}	2.4996×10^{-3}	1.0044	1.7449×10^{-7}
32	0.04619	1.0069×10^{-5}	8.8158×10^{-4}	1.0041	4.1236×10^{-8}
64	0.02310	2.5211×10^{-6}	3.1033×10^{-4}	1.0026	6.5926×10^{-9}

The eigenvalue error again approaches second-order convergence. The recovered-gradient errors decrease at a rate approaching 1.5, and the estimator effectivity index approaches one. The postprocessed eigenvalue error is smaller than the original error at every tested level, although its observed rates are not uniform. The results provide additional validation for one smoothly perturbed mesh family; they do not establish analogous behavior on arbitrary unstructured or strongly graded triangulations.

4.7 Numerical Validation on a Rectangular Domain

To further examine the performance of the proposed recovery method under a different domain geometry, an additional numerical experiment is conducted on the rectangular domain

$$\Omega = (0,2) \times (0,1), \qquad \kappa = 1.$$

For this domain, an analytical eigenfunction is given by

$$u(x,y) = C\cosh(a(x-1))\cosh\left(b\left(y - \frac{1}{2}\right)\right),$$

where the positive parameters a and b satisfy

$$a^2 + b^2 = 1, \qquad a\tanh(a) = b\tanh\left(\frac{b}{2}\right).$$

Consequently, the corresponding first eigenvalue is

$$\lambda_{\mathrm{rect}} = a\tanh(a) = b\tanh\left(\frac{b}{2}\right) \approx 0.310510269429546.$$

Numerically,

$$a \approx 0.5877671962, \qquad b \approx 0.8090301126.$$

The constant C is determined by the boundary normalization $\|u\|_{L^2(\partial\Omega)} = 1$:

$$C^{-2} = 2\cosh^2(a)\left(\frac{1}{2} + \frac{\sinh(b)}{2b}\right) + 2\cosh^2\left(\frac{b}{2}\right)\left(1 + \frac{\sinh(2a)}{2a}\right).$$

This gives $C \approx 0.3492063842$.

The relation $a^2 + b^2 = 1$ ensures that the eigenfunction satisfies the differential equation in the interior, while the second relation guarantees the same Robin eigenvalue on all four sides.

The rectangular domain is divided into $2n \times n$ congruent squares, and each square is split into two triangles along the same diagonal. With $\ell = 1/n$, the maximum element diameter is

$$h = \sqrt{2}\ell = \frac{\sqrt{2}}{n}.$$

The mesh parameters are

$$n = 4,\ 8,\ 16,\ 32,\ 64,\ 128.$$

The same continuous piecewise linear finite element discretization and equal-weight nodal averaging recovery operator as in the unit-square experiments are employed. The numbers of nodes and triangles are $(2n+1)(n+1)$ and $4n^2$, respectively.

The eigenvalue error, recovery-based estimator, and effectivity index are defined by

$$E_h = |\lambda_h - \lambda_{\mathrm{rect}}|, \qquad \eta_h^2 = \|G_h u_h - \nabla u_h\|_{0,\Omega}^2, \qquad R_h = \frac{\eta_h^2}{E_h}.$$

Table 4.7: Eigenvalue errors and recovery-based estimator on the rectangular domain

n	Nodes	Elements	h	λ_h	E_h	Rate	η_h^2	Rate	R_h
4	45	64	0.353553	0.3113116013	8.0133×10^{-4}	–	7.8409×10^{-4}	–	0.97848
8	153	256	0.176777	0.3107159586	2.0569×10^{-4}	1.9619	2.0559×10^{-4}	1.9313	0.99951
16	561	1024	0.088388	0.3105621600	5.1891×10^{-5}	1.9869	5.2091×10^{-5}	1.9806	1.00387
32	2145	4096	0.044194	0.3105232796	1.3010×10^{-5}	1.9958	1.3053×10^{-5}	1.9967	1.00328
64	8385	16384	0.022097	0.3105135248	3.2554×10^{-6}	1.9987	3.2621×10^{-6}	2.0005	1.00205
128	33153	65536	0.011049	0.3105110835	8.1406×10^{-7}	1.9996	8.1499×10^{-7}	2.0009	1.00114

As shown in Table 4.7, both the eigenvalue error and the recovery-based estimator exhibit approximately second-order convergence. Their observed convergence orders approach 2 as the mesh is refined. Moreover, the effectivity index R_h approaches 1. In particular, its value on the finest mesh is 1.00114. These results provide numerical evidence of the asymptotic exactness of the recovery-based error estimator on the rectangular domain.

To further examine the gradient approximation and the postprocessed eigenvalue, the following quantities are defined:

$$E_{\mathrm{FEM},h} = \|\nabla u_h - \nabla u\|_{0,\Omega},$$
$$E_{\mathrm{rec},h} = \|G_h u_h - \nabla u\|_{0,\Omega},$$
$$\widehat{\lambda}_h = \lambda_h - \eta_h^2.$$

Table 4.8: Gradient errors and postprocessed eigenvalue errors on the rectangular domain

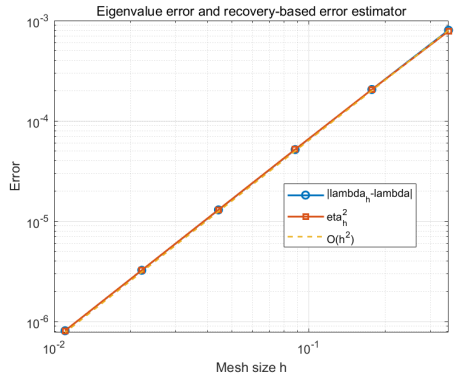
n	$E_{\mathrm{FEM},h}$	Rate	$E_{\mathrm{rec},h}$	Rate	$\lvert\widehat{\lambda}_h - \lambda_{\mathrm{rect}}\rvert$	Rate
4	2.833893×10^{-2}	–	2.048708×10^{-2}	–	1.724484×10^{-5}	–
8	1.434763×10^{-2}	0.9820	7.475540×10^{-3}	1.4545	1.016431×10^{-7}	7.4065
16	7.204370×10^{-3}	0.9939	2.670512×10^{-3}	1.4851	2.005693×10^{-7}	-0.9806
32	3.607081×10^{-3}	0.9980	9.456162×10^{-4}	1.4978	4.271089×10^{-8}	2.2314
64	1.804289×10^{-3}	0.9994	3.338631×10^{-4}	1.5019	6.665992×10^{-9}	2.6797
128	9.022554×10^{-4}	0.9998	1.178391×10^{-4}	1.5025	9.282414×10^{-10}	2.8442

The unusually large rate at the first refinement is not interpreted as an asymptotic convergence order. The negative rate records the increase in the measured error from $n = 8$ to $n = 16$.

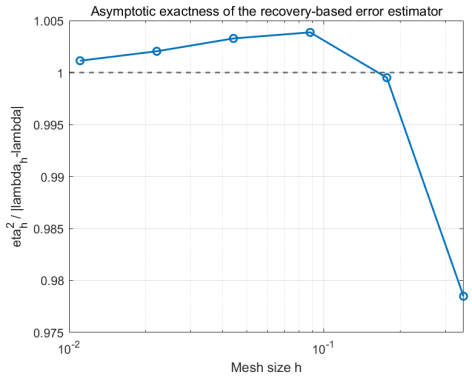
The finite element gradient error approaches first-order convergence, whereas the recovered gradient error approaches order 1.5. On the finest mesh, the two errors are 9.022554×10^{-4} and 1.178391×10^{-4}, respectively. This behavior is consistent with the predicted gradient recovery convergence rate.

The postprocessed eigenvalue error is smaller than the original eigenvalue error at all tested mesh levels, but it is not monotone. In particular, it increases from 1.016431×10^{-7} at $n = 8$ to 2.005693×10^{-7} at $n = 16$. The corresponding negative observed rate is retained because it correctly reflects this increase. The later rates do not, by themselves, establish a stable asymptotic convergence order for the postprocessed eigenvalue.

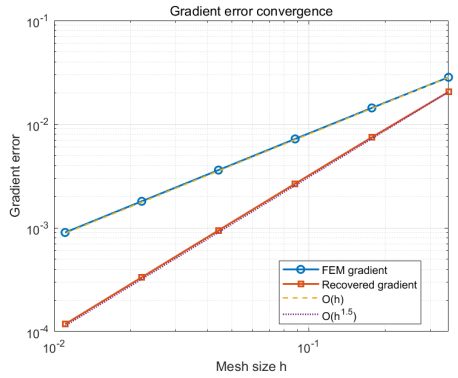
The four panels in Figure 4.5 summarize the eigenvalue error, estimator effectivity, gradient errors, and postprocessed eigenvalue error.



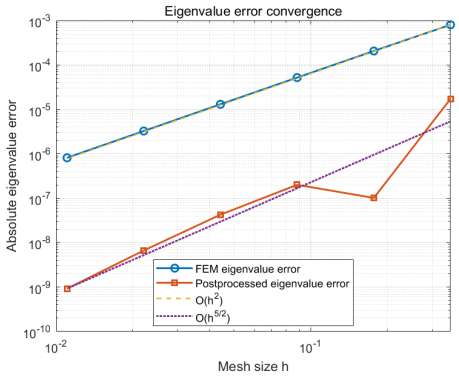
(a) Eigenvalue error and estimator



(b) Effectivity index



(c) Gradient errors



(d) Postprocessed eigenvalue error

Figure 4.5: Numerical results on the rectangular domain: (a) eigenvalue error and recovery-based estimator; (b) effectivity index; (c) finite element and recovered-gradient errors; (d) postprocessed eigenvalue error.

The results on the rectangular domain provide an additional numerical test of the proposed recovery procedure under a different domain geometry. Together with the experiments on the unit square and the smoothly perturbed nonuniform meshes, they support the observed convergence behavior for the tested domain and mesh families. They do not establish the same behavior for arbitrary polygonal domains or strongly graded and unstructured meshes.

4.8 Section Summary

Numerical experiments on the unit square demonstrate that the finite element eigenvalue error converges at approximately second order, while the original and recovered gradient errors exhibit convergence orders close to 1 and 1.5, respectively. The recovery-based error estimator also shows approximately second-order convergence, and its effectivity index approaches 1 as the mesh is refined.

Additional experiments on smoothly perturbed nonuniform triangular meshes provide further numerical validation of the proposed recovery method. The eigenvalue error again exhibits approximately second-order convergence, while the recovered-gradient error approaches an order of 1.5.

Furthermore, the experiment on the rectangular domain $\Omega = (0, 2) \times (0, 1)$ confirms similar convergence behavior on a domain with a different aspect ratio. The eigenvalue error and the squared recovery-based estimator exhibit approximately second-order convergence, the recovered-gradient

error approaches order 1.5, and the effectivity index approaches 1.

The postprocessed eigenvalue error is smaller than the original eigenvalue error in the tested cases, although its convergence behavior is nonmonotone. Overall, the numerical results provide additional evidence supporting the theoretical analysis for the tested domain geometries and mesh families. Further investigation is required for more general polygonal domains and strongly graded or unstructured meshes.

5 Conclusions and Future Work

5.1 Conclusions

This paper investigates a simple-averaging gradient recovery method and its application to error estimation for the Steklov eigenvalue problem using continuous piecewise linear finite elements. A recovered gradient is constructed by assigning equal weights to the elementwise gradients in each nodal patch. Based on this recovery operator, a computable error estimator is developed, and its superconvergence properties and relationship with the eigenvalue error are analyzed. The main conclusions are summarized as follows.

(1) The variational formulation and finite element approximation of the Steklov eigenvalue problem are established. A priori error estimates for the discrete eigenfunction and eigenvalue are derived, and an eigenvalue error identity is obtained under boundary L^2 normalization. This identity shows that the squared gradient error provides the leading contribution to the eigenvalue error, thereby motivating the recovery-based estimation developed in this paper.

(2) A simple equal-weight nodal averaging recovery operator is constructed. At each mesh node, the recovered gradient is defined as the arithmetic average of the elementwise gradients over its nodal patch, and a continuous piecewise linear recovered gradient field is obtained through nodal interpolation. Under the prescribed mesh-structure and regularity assumptions, the recovered gradient satisfies the superconvergence estimate

$$\|G_h u_h - \nabla u\|_{0,\Omega} \le C h^{1+\alpha_0}.$$

Based on this result, the recovery-based error estimator is defined by

$$\eta_h = \|G_h u_h - \nabla u_h\|_{0,\Omega}.$$

Combining the superconvergence estimate with the eigenvalue error identity yields

$$\lambda_h - \lambda = \eta_h^2 + O(h^{2+\alpha_0}).$$

Furthermore, for the first isolated simple Steklov eigenvalue, under the additional nondegeneracy condition $\lambda_h - \lambda \ge c_0 h^2$, the estimator is asymptotically exact:

$$\frac{\eta_h^2}{\lambda_h - \lambda} = 1 + O(h^{\alpha_0}).$$

The corresponding postprocessed eigenvalue, defined by

$$\widehat{\lambda}_h = \lambda_h - \eta_h^2,$$

satisfies

$$|\widehat{\lambda}_h - \lambda| \le C h^{2+\alpha_0}.$$

(3) Numerical experiments are conducted on the unit square with uniform and smoothly perturbed structured nonuniform triangular meshes, and on an additional rectangular domain with uniform triangular meshes. On uniform meshes on both domains, the finite element eigenvalue error exhibits approximately second-order convergence, while the original and recovered gradient errors approach convergence orders of 1 and 1.5, respectively. The squared recovery-based estimator η_h^2 also exhibits

approximately second-order convergence, and its effectivity index approaches 1 as the mesh is refined.

Additional experiments on smoothly perturbed nonuniform meshes on the unit square show similar qualitative convergence behavior. These numerical results provide further evidence supporting the theoretical superconvergence and asymptotic exactness results for the tested domain geometries and mesh families.

The postprocessed eigenvalue error is smaller than the corresponding original finite element eigenvalue error in the tested cases. However, its convergence behavior is nonmonotone, and the observed convergence orders do not yet establish a stable asymptotic rate. Thus, the numerical results demonstrate an improvement in eigenvalue accuracy while leaving its detailed asymptotic behavior for further investigation.

5.2 Limitations and Future Work

The present analysis relies on sufficient solution regularity and structured-mesh assumptions, including shape regularity, quasi-uniformity, and the approximate parallelogram condition at regular interior nodes. The numerical experiments cover two polygonal domains: the unit square and the rectangular domain $\Omega = (0, 2) \times (0, 1)$. On the unit square, both uniform and smoothly perturbed structured nonuniform triangular meshes are considered, whereas uniform triangular meshes are used on the rectangular domain. These experiments provide numerical evidence for the tested domain geometries and mesh families only. Further investigation is needed to establish the performance of the proposed recovery method on more general polygonal domains, strongly graded meshes, and unstructured triangulations. Future work will also investigate domains with reduced regularity, adaptive refinement based on recovery indicators, higher-order finite elements, and extensions to other elliptic eigenvalue problems.

Competing Interests

Authors have declared that no competing interests exist.

References

Armentano, M. G. and Padra, C. (2008). A posteriori error estimates for the Steklov eigenvalue problem. *Applied Numerical Mathematics*, 58(5):593–601. https://doi.org/10.1016/j.apnum.2007.01.011.

Bi, H., Yang, Y., Yu, Y., and Han, J. (2018). New error estimates for linear triangle finite elements in the Steklov eigenvalue problem. *Journal of Computational Mathematics*, 36(5):682–692. https://doi.org/10.4208/jcm.1703-m2014-0188.

Boffi, D. (2010). Finite element approximation of eigenvalue problems. *Acta Numerica*, 19:1–120. https://doi.org/10.1017/S0962492910000012.

Hlaváček, I., Křížek, M., and Pištora, V. (1996). How to recover the gradient of linear elements on nonuniform triangulations. *Applications of Mathematics*, 41(4):241–267. https://doi.org/10.21136/AM.1996.134325.

Li, H. and Zhang, Y. (2024). An adaptive algorithm for Steklov eigenvalues of the Lamé operator in linear elasticity. *Computational and Applied Mathematics*, 43(4):210. https://doi.org/10.1007/s40314-024-02736-0.

Mao, D., Shen, L., and Zhou, A. (2006). Adaptive finite element algorithms for eigenvalue problems based on local averaging type a posteriori error estimates. *Advances in Computational Mathematics*, 25(1–3):135–160. https://doi.org/10.1007/s10444-004-7617-0.

Naga, A., Zhang, Z., and Zhou, A. (2006). Enhancing eigenvalue approximation by gradient recovery. *SIAM Journal on Scientific Computing*, 28(4):1289–1300. https://doi.org/10.1137/050640588.

Xiong, C., Xie, M., Luo, F., and Su, H. (2023). A posteriori and superconvergence error analysis for finite element approximation of the Steklov eigenvalue problem. *Computers & Mathematics with Applications*, 144:90–99. https://doi.org/10.1016/j.camwa.2023.05.025.

Xu, J. and Zhang, Z. (2004). Analysis of recovery type a posteriori error estimators for mildly structured grids. *Mathematics of Computation*, 73(247):1139–1152. https://doi.org/10.1090/S0025-5718-03-01600-4.

Zhang, J. and Han, J. (2025). Asymptotically exact a posteriori error estimates for non-symmetric eigenvalue problems. *Journal of Mathematical Research with Applications*, 45(3):411–426. https://doi.org/10.3770/j.issn:2095-2651.2025.03.008.

Zienkiewicz, O. C. and Zhu, J. Z. (1992). The superconvergent patch recovery and a posteriori error estimates. Part 1: The recovery technique. *International Journal for Numerical Methods in Engineering*, 33(7):1331–1364. https://doi.org/10.1002/nme.1620330702.